*Meccanica* **35:** 443–456, 2000.


# Analysis of Two Collinear Cracks in a Piezoelectric Layer Bonded to Two Half Spaces Subjected to Anti-plane Shear

ZHEN-GONG ZHOU, JUN-YING CHEN and BIAO WANG
*Harbin Institute of Technology, Center for Composite Materials and Electro-Optics Research Center, P.O. Box 1247; Harbin 150001, P.R. China*

(Received: 10 July 2000; accepted in revised form: 5 February 2001)

**Abstract.** In this paper, the behavior of two collinear anti-plane shear cracks in a piezoelectric layer bonded to two half spaces is investigated by a new method for the impermeable crack face conditions. The cracks are parallel to the interfaces in the mid-plane of the piezoelectric layer. By using the Fourier transform, the problem can be solved with two pairs of triple integral equations. These equations are solved using the Schmidt method. This process is quite different from that adopted previously. Numerical examples are provided to show the effect of the geometry of the interacting cracks and the piezoelectric constants of the material upon the stress intensity factor of the cracks.

**Sommario.** In questo lavoro si esamina il comportamento di due fessure di taglio antipiane collineari in uno strato di materiale piezoelettrico aderente a due semispazi, mediante un nuovo metodo per le condizioni di superficie impermeabile della fessura. Le fessure sono parallele alle interfacce nel piano medio dello strato piezoelettrico. Usando la trasformata di Fourier, il problema può essere risolto con due coppie di equazioni integrali triple, che vengono risolte con il metodo di Schmidt. La procedura è sostanzialmente differente da quella adottata in precedenza. Vengono presentati numerosi esempi per evidenziare l' effetto della geometria delle fessure interagenti e delle costanti piezoelettriche del materiale sul fattore di concentrazione delle tensioni nelle fessure.

**Key words:** Piezoelectric materials, Triple integral equations, Fourier transform, Collinear cracks, Mechanics of fracture.

## 1. Introduction

It is well known that piezoelectric materials produce an electric field when deformed and undergo deformation when subjected to an electric field. The coupling nature of piezoelectric materials has attracted wide applications in electric-mechanical and electric devices, such as electric-mechanical actuators, sensors and structures. When subjected to mechanical and electrical loads in service, these piezoelectric materials can fail prematurely due to defects, for example cracks, holes, etc. arising during their manufacturing process. Therefore, it is of great importance to study the electro–elastic interaction and fracture behavior of piezoelectric materials. Moreover, it is known that the failure of solids results from the cracks, and in most cases, the unstable growth of the crack is brought about by the external loads. So, the study of the fracture mechanics of piezoelectric materials is much more important in recent research.

In the theoretical studies of crack problems, several different electric boundary conditions at the crack surfaces have been proposed by numerous researchers. For example, for the sake of analytical simplification, the assumption that the crack surfaces are impermeable to electric fields was adopted by [1–13, etc.]. In this model, the assumption of the impermeable cracks refers to the fact that the crack surfaces are free of surface charge and thus the electric displacement vanishes within the crack. In fact, cracks in piezoelectric materials consist of vacuum, air or some other gas. This requires that the electric fields can propagate through the crack, so the electric displacement component perpendicular to the crack surfaces should be continuous across the crack surfaces. Along this line, [14] analyzed crack problems in piezoelectric materials. In this case, the electric displacement does not exhibit the singularity behavior at the crack tip, whereas it has the inverse square root singularity at the crack tip for an impermeable crack. In addition, usually the conducting cracks which are filled with conducting gas or liquid are also applied to be a kind of simplified cracks models in piezoelectric materials by many researchers, such as [15, 16]. Recently, [17–19] avoided the common assumption of electric impermeability and utilized more accurate electric boundary conditions at the rim of an elliptical flaw to deal with anti-plane problems in piezoelectricity. They analyzed the effects of electric boundary conditions at the crack surfaces on the fracture mechanics of piezoelectric materials. However, due to much simpler treatment from a mathematical point of view, the impermeable crack and the conducting crack are still employed extensively in the study of the crack problems of piezoelectric materials. In particular, control of laminated structures including piezoelectric devices was the subject of research by [20–23]. Many piezoelectric devices comprise both piezoelectric and structural layers, and an understanding of the fracture process of piezoelectric structural systems is of great importance in order to ensure the structural integrity of piezoelectric devices [10, 24, 25]. To our knowledge, the electro-elastic behavior of laminated piezoelectric composite structures with two impermeable cracks has not been studied despite the fact that many piezoelectric devices are constructed in a laminated form. Accordingly, there is a need to investigate the electro–elastic fracture mechanics analysis of laminated piezoelectric structures.

In the present paper, we consider the anti-plane shear problem for two cracked piezoelectric layer bonded to two half spaces for the impermeable crack face conditions. The two half spaces have similar properties and the piezoelectric laminate is subjected to combined mechanical and electrical loads. The cracks are situated symmetrically and oriented in the direction parallel to the interfaces of the layer. The interaction between two collinear symmetrical cracks subjects to anti-plane shear in piezoelectric layer bonded to two half spaces is investigated using the Schmidt method [26]. It is a simple and convenient method for solving this problem. Fourier transform is applied and a mixed boundary value problem is reduced to two pairs of triple integral equations. In solving the triple integral equations, the crack surface displacement and electric potential are expanded in a series of Jacobi polynomials. This process is quite different from that adopted in previous works [1, 3, 6–8, 10, 18, 27–30]. The form of solution is easy to understand. Numerical calculations are carried out for the stress intensity factors.

## 2. Formulation of the Problem

Consider a piezoelectric layer that is sandwiched between two elastic half planes with an elastic stiffness constant $c_{44}^E$. Quantities in the half spaces will subsequently be designated by superscript $E$. The piezoelectric material layer of thickness $2h$ contains two cracks of length $1$-$b$ that are situated in the mid-plane and are parallel to the interfaces, as shown in Figure 1. $2b$ is the distance between the cracks (The solution of the piezoelectric layer of width $2h$ containing two collinear Griffith cracks of length $a$–$b$ can easily be obtained by a simple change in the numerical values of the present paper $a > b > 0$). The piezoelectric boundary-value problem for anti-plane shear [11] is considerably simplified if we consider only the

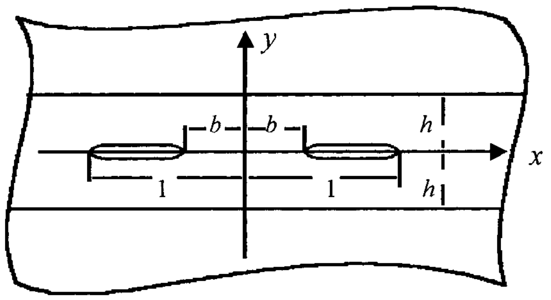


*Figure 1.* Cracks in a piezoelectric layer under anti-plane shear.

out-of-plane displacement and the in-plane electric fields. The plate is subjected to a constant stress $\tau_{yz} = -\tau_0$, and a constant electric displacement $D_y = -D_0$ along the surface of the cracks, such that the constitutive equations can be written as

$$\tau_{zk} = c_{44}w_{,k} + e_{15}\phi_{,k} \qquad (k = 1, 2), \tag{1}$$

$$D_k = e_{15}w_{,k} - \varepsilon_{11}\phi_{,k} \qquad (k = 1, 2), \tag{2}$$

$$\tau^E_{xz} = c^E_{44}w^E_{,x}, \tag{3}$$

$$\tau^E_{yz} = c^E_{44}w^E_{,y}, \tag{4}$$

where $\tau_{zk}$, $D_k(k = x, y)$ are the anti-plane shear stress and in-plane electric displacement, respectively; $c_{44}$, $e_{15}$, $\varepsilon_{11}$ are the shear modulus, piezoelectric coefficient and dielectric parameter, respectively; $w$ and $\phi$ are the mechanical displacement and electric potential. $\tau^E_{xz}$, $\tau^E_{yz}$ and $w^E$ are the shear stress, and the displacement in the half elastic spaces, respectively.
The anti-plane governing equations are

$$c_{44}\nabla^2 w + e_{15}\nabla^2\phi = 0, \tag{5}$$

$$e_{15}\nabla^2 w - \varepsilon_{11}\nabla^2\phi = 0, \tag{6}$$

$$\nabla^2 w^E = 0, \tag{7}$$

where $\nabla^2 = \partial^2/\partial x^2 + \partial^2/\partial y^2$ is the two-dimensional Laplace operator. Body force, other than inertia, and the free charge are ignored in the present work. Because of the assumed symmetry in geometry and loading, it is sufficient to consider the problem for $0 \leqslant x < \infty$, $0 \leqslant y < \infty$ only. Substitute (6) into (5) to give $\nabla^2 w = 0$, provided $(c_{44} + e^2_{15}/\varepsilon_{11}) \neq 0$. The solutions in Fourier transform are

$$w(x, y) = \frac{2}{\pi}\int_0^\infty [A_1(s)e^{-sy} + A_2(s)e^{sy}]\cos(sx)\,\mathrm{d}s, \tag{8}$$

$$w^E(x, y) = \frac{2}{\pi}\int_0^\infty A_3(s)e^{-sy}\cos(sx)\,\mathrm{d}s, \tag{9}$$

where $A_1(s)$, $A_2(s)$ and $A_3(s)$ are unknown functions, and a superposed bar indicates the Fourier transform throughout the paper, for example,

$$\overline{f}(s) = \int_{-\infty}^{\infty} f(x)e^{-isx}\,\mathrm{d}x. \tag{10}$$

Inserting (8) into (6) gives

$$\phi(x, y) - \frac{e_{15}}{\varepsilon_{11}} w(x, y) = \frac{2}{\pi}\int_0^{\infty} [B_1(s)e^{-sy}\,\mathrm{d}s + B_2(s)e^{sy}]\cos(sx)\,\mathrm{d}s, \tag{11}$$

where $B_1(s)$ and $B_2(s)$ are unknown functions. The boundary conditions of the present problem are:

$$\tau_{yz}(x, 0) = -\tau_0, \qquad b \leqslant |x| \leqslant 1 \tag{12}$$

$$D_y(x, 0) = -D_0, \qquad b \leqslant |x| \leqslant 1 \tag{13}$$

$$w(x, 0) = \phi(x, 0) = 0, \qquad |x| < b, |x| > 1, \tag{14}$$

$$\tau_{yz}(x, h) = \tau_{yz}^E(x, h), \tag{15}$$

$$w(x, \pm h) = w^E(x, \pm h), \tag{16}$$

$$D_y(x, \pm h) = 0, \tag{17}$$

$$w(x, y) = w^E(x, y) = \phi(x, y) = 0, \quad \text{for} \quad \sqrt{x^2 + y^2} \to \infty. \tag{18}$$

The boundary conditions can be applied to yield two pairs of triple integral equations:

$$\frac{2}{\pi}\int_0^{\infty} A(s)\cos(sx)\,\mathrm{d}s = 0, \qquad 0 \leqslant x < b, \qquad 1 < x, \tag{19}$$

$$\frac{2}{\pi}\int_0^{\infty} sF_1(s)A(s)\cos(sx)\,\mathrm{d}s = \frac{1}{\mu}\left(\tau_0 + \frac{e_{15}D_0}{\varepsilon_{11}}\right), \qquad b \leqslant x \leqslant 1 \tag{20}$$

and

$$\frac{2}{\pi}\int_0^{\infty} B(s)\cos(sx)\,\mathrm{d}s = 0, \qquad 0 \leqslant x < b, 1 < x, \tag{21}$$

$$\frac{2}{\pi}\int_0^{\infty} sF_2(s)B(s)\cos(sx)\,\mathrm{d}s = -\frac{D_0}{\varepsilon_{11}}, \qquad b \leqslant x \leqslant 1, \tag{22}$$

where

$$F_1(s) = \frac{1-\mu_3 e^{-2sh}}{1+\mu_3 e^{-2sh}}, \qquad F_2(s) = \frac{1-e^{-2sh}}{1+e^{-2sh}}, \qquad A(s) = (1+\mu_3 e^{-2sh})A_1(s),$$

$$A_2(s) = \mu_3 e^{-2sh} A_1(s), \qquad B(s) = (1+e^{-2sh})B_1(s), \qquad B_2(s) = e^{-2sh} B_1(s),$$

$$\mu = c_{44} + \frac{e_{15}^2}{\varepsilon_{11}}, \qquad \mu_1 = 1 - \frac{c_{44}^E}{\mu}, \qquad \mu_2 = 1 + \frac{c_{44}^E}{\mu}, \qquad \mu_3 = \frac{\mu_1}{\mu_2}.$$

To determine the unknown functions $A(s)$, $B(s)$, the above two pairs of triple integral equations (19–22) must be solved.

## 3. Solution of the Triple Integral Equation

The Schmidt method [26] is used to solve the triple integral equations. The displacement $w$ and the electric potential $\phi$ are represented by the following series:

$$\begin{aligned} w(x,0) &= \sum_{n=0}^{\infty} a_n P_n^{(\frac{1}{2},\frac{1}{2})}\left(\frac{x-\frac{1+b}{2}}{\frac{1-b}{2}}\right) \\ &\quad \times \left(1 - \frac{\left(x-\frac{1+b}{2}\right)^2}{\left(\frac{1-b}{2}\right)^2}\right)^{\frac{1}{2}}, \quad \text{for} \quad b \leqslant x \leqslant 1, \quad y = 0, \end{aligned} \tag{23}$$

$$w(x,0) = 0, \quad \text{for} \quad x < b, \qquad x > 1, \qquad y = 0, \tag{24}$$

$$\begin{aligned} \phi(x,0) &= \sum_{n=0}^{\infty} b_n P_n^{(\frac{1}{2},\frac{1}{2})}\left(\frac{x-\frac{1+b}{2}}{\frac{1-b}{2}}\right) \\ &\quad \times \left(1 - \frac{\left(x-\frac{1+b}{2}\right)^2}{\left(\frac{1-b}{2}\right)^2}\right)^{\frac{1}{2}}, \quad \text{for} \quad b \leqslant x \leqslant 1, \qquad y = 0, \end{aligned} \tag{25}$$

$$\phi(x,0) = 0, \quad \text{for} \quad x < b, \qquad x > 1, \qquad y = 0, \tag{26}$$

where $a_n$ and $b_n$ are unknown coefficients to be determined and $P_n^{(1/2,1/2)}(x)$ is a Jacobi polynomial [31]. The Fourier transform of (23) and (25) is [32]

$$A(s) = \bar{w}(s,0) = \sum_{n=0}^{\infty} a_n Q_n G_n(s) \frac{1}{s} J_{n+1}\left(s\frac{1-b}{2}\right), \tag{27}$$

$$B(s)=\overline{\phi}(s,0)-\frac{e_{15}}{\varepsilon_{11}}\bar{w}(s,0)=\sum_{n=0}^{\infty}(b_n-\frac{e_{15}}{\varepsilon_{11}}a_n)Q_nG_n(s)\frac{1}{s}J_{n+1}\left(s\frac{1-b}{2}\right), \tag{28}$$

$$Q_n=2\sqrt{\pi}\frac{\Gamma\left(n+1+\frac{1}{2}\right)}{n!}, \tag{29}$$

$$G_n(s)=\begin{cases}(-1)^{\frac{n}{2}}\cos\left(s\frac{1+b}{2}\right), & n=0,2,4,6,\dots,\\ (-1)^{\frac{n-1}{2}}\sin\left(s\frac{1+b}{2}\right), & n=1,3,5,7,\dots,\end{cases} \tag{30}$$

where $\Gamma(x)$ and $J_n(x)$ are the Gamma and Bessel functions, respectively.

Substituting (27) and (28) into equations (19–22) satisfies (19) and (21). After integration with respect to $x$ in $[b,x]$ , (20) and (22) reduce to

$$\sum_{n=0}^{\infty}a_nQ_n\int_0^{\infty}s^{-1}G_n(s)\,J_{n+1}\left(s\frac{1-b}{2}\right)\{1+[F_1(s)-1]\}[\sin(sx)-\sin(sb)]\,\mathrm{d}s$$
$$=\frac{\pi}{2\mu}\tau_0(1+\lambda)(x-b), \tag{31}$$

$$\sum_{n=0}^{\infty}\left(b_n-\frac{e_{15}}{\varepsilon_{11}}a_n\right)Q_n\int_0^{\infty}s^{-1}G_n(s)\,J_{n+1}\left(s\frac{1-b}{2}\right)$$
$$\times\{1+[F_2(s)-1]\}[\sin(sx)-\sin(sb)]\,\mathrm{d}s$$
$$=-\frac{\pi D_0}{2\varepsilon_{11}}(x-b), \tag{32}$$

where $\lambda=\dfrac{e_{15}D_0}{\varepsilon_{11}\tau_0}$.

The semi-infinite integral in (31) and (32) can be modified as [31]

$$\int_0^{\infty}\frac{1}{s}J_{n+1}\left(s\frac{1-b}{2}\right)\{1+[F_1(s)-1]\}\cos\left(s\frac{1+b}{2}\right)\sin(sx)\,\mathrm{d}s$$
$$=\frac{1}{2(n+1)}\left\{\frac{\left(\frac{1-b}{2}\right)^{n+1}\sin\left(\frac{(n+1)\pi}{2}\right)}{\left\{x+\frac{1+b}{2}+\sqrt{\left(x+\frac{1+b}{2}\right)^2-\left(\frac{1-b}{2}\right)^2}\right\}^{n+1}}\right.$$
$$\left.-\sin\left[(n+1)\sin^{-1}\left(\frac{1+b-2x}{1-b}\right)\right]\right\}$$
$$+\int_0^{\infty}\frac{1}{s}[F_1(s)-1]J_{n+1}\left(s\frac{1-b}{2}\right)\cos\left(s\frac{1+b}{2}\right)\sin(sx)\,\mathrm{d}s \tag{33}$$

$$\int_0^\infty \frac{1}{s} J_{n+1}\left(s\frac{1-b}{2}\right)\{1+[F_1(s)-1]\}\sin\left(s\frac{1+b}{2}\right)\sin(sx)\,\mathrm{d}s$$

$$= \frac{1}{2(n+1)}\left\{\cos\left[(n+1)\sin^{-1}\left(\frac{1+b-2x}{1-b}\right)\right]\right.$$

$$\left. - \frac{\left(\frac{1-b}{2}\right)^{n+1}\cos\left(\frac{(n+1)\pi}{2}\right)}{\left\{x+\frac{1+b}{2}+\sqrt{\left(x+\frac{1+b}{2}\right)^2-\left(\frac{1-b}{2}\right)^2}\right\}^{n+1}}\right\}$$

$$+ \int_0^\infty \frac{1}{s}[F_1(s)-1]J_{n+1}\left(s\frac{1-b}{2}\right)\sin\left(s\frac{1+b}{2}\right)\sin(sx)\,\mathrm{d}s. \tag{34}$$

For large $s$, the integrands of the semi-infinite integral in (33) and (34) have exponential form, so that they can be evaluated numerically by Filon's method [33]. Thus the semi-infinite integral in (31) and (32) can be evaluated directly. Equations (31) and (32) can now be solved for the coefficients $a_n$ and $b_n$ by the Schmidt method [26]. For brevity, (31) can be rewritten as ((32) can be solved using similar method)

$$\sum_{n=0}^{\infty} a_n E_n(x) = U(x), b < x < 1, \tag{35}$$

where $E_n(x)$ and $U(x)$ are known functions and coefficients $a_n$ are to be determined. A set of functions $P_n(x)$ which satisfy the orthogonality condition

$$\int_b^1 P_m(x)P_n(x)\,\mathrm{d}x = N_n\delta_{mn}, \qquad N_n = \int_b^1 P_n^2(x)\,\mathrm{d}x \tag{36}$$

can be constructed from the function, $E_n(x)$, such that

$$P_n(x) = \sum_{i=0}^{n} \frac{M_{in}}{M_{nn}} E_i(x), \tag{37}$$

where $M_{in}$ is the cofactor of the element $d_{in}$ of $D_n$ , which is defined as

$$D_n = \begin{bmatrix} d_{00}, d_{01}, d_{02}, \ldots, d_{0n} \\ d_{10}, d_{11}, d_{12}, \ldots, d_{1n} \\ d_{20}, d_{21}, d_{22}, \ldots, d_{2n} \\ \ldots\ldots\ldots\ldots\ldots\ldots \\ \ldots\ldots\ldots\ldots\ldots\ldots \\ \ldots\ldots\ldots\ldots\ldots\ldots \\ d_{n0}, d_{n1}, d_{n2}, \ldots, d_{nn} \end{bmatrix}, \qquad d_{ij} = \int_b^1 E_i(x)E_j(x)\,\mathrm{d}x. \tag{38}$$

Using (35–38), we obtain

$$a_n = \sum_{j=n}^{\infty} q_j \frac{M_{nj}}{M_{jj}} \tag{39}$$

with

$$q_j = \frac{1}{N_j} \int_b^1 U(x) P_j(x)\, \mathrm{d}x. \tag{40}$$

## 4. Intensity Factors

Although we can determine the entire stress field and the electric displacement from coefficients $a_n$ and $b_n$ , it is of importance in fracture mechanics to determine the stress $\tau_{yz}$ and the electric displacement $D_y$ in the vicinity of the crack tips. $\tau_{yz}$ and $D_y$ along the crack line can be expressed as

$$\begin{aligned} \tau_{yz}(x,0) &= -\frac{2\mu}{\pi}\sum_{n=0}^{\infty} a_n Q_n \int_0^{\infty} G_n(s)\{1+[F_1(s)-1]\} J_{n+1}\left(s\frac{1-b}{2}\right)\cos(xs)\,\mathrm{d}s \\ &\quad -\frac{2e_{15}}{\pi}\sum_{n=0}^{\infty}\left(b_n - \frac{e_{15}}{\varepsilon_{11}}a_n\right) Q_n \int_0^{\infty} G_n(s)\{1+[F_2(s)-1]\} \\ &\quad \times J_{n+1}\left(s\frac{1-b}{2}\right)\cos(xs)\,\mathrm{d}s, \end{aligned} \tag{41}$$

$$\begin{aligned} D_y(x,0) &= \frac{2}{\pi}\sum_{n=0}^{\infty}(\varepsilon_{11}b_n - e_{15}a_n) Q_n \int_0^{\infty} G_n(s)\{1+[F_2(s)-1]\} \\ &\quad \times J_{n+1}\left(s\frac{1-b}{2}\right)\cos(xs)\,\mathrm{d}s. \end{aligned} \tag{42}$$

An examination of (41) and (42) shows that the singular part of the stress field and electric displacement can be obtained from [31]

$$\cos\left(s\frac{1+b}{2}\right)\cos(sx) = \frac{1}{2}\left\{\cos\left[s\left(\frac{1+b}{2}-x\right)\right] + \cos\left[s\left(\frac{1+b}{2}+x\right)\right]\right\},$$

$$\sin\left(s\frac{1+b}{2}\right)\cos(sx) = \frac{1}{2}\left\{\sin\left[s\left(\frac{1+b}{2}-x\right)\right] + \sin\left[s\left(\frac{1+b}{2}+x\right)\right]\right\},$$

$$\int_0^{\infty} J_n(sa)\cos(bs)\,\mathrm{d}s = \begin{cases} \dfrac{\cos[n\sin^{-1}(b/a)]}{\sqrt{a^2-b^2}}, & a > b, \\ -\dfrac{a^n \sin(n\pi/2)}{\sqrt{b^2-a^2}[b+\sqrt{b^2-a^2}]^n}, & b > a, \end{cases}$$

$$\int_0^\infty J_n(sa)\sin(bs)\,\mathrm{d}s = \begin{cases} \dfrac{\sin[n\sin^{-1}(b/a)]}{\sqrt{a^2-b^2}}, & a > b, \\ \dfrac{a^n\cos(n\pi/2)}{\sqrt{b^2-a^2}[b+\sqrt{b^2-a^2}]^n}, & b > a. \end{cases}$$

The singular part of the stress field and electric displacement can be expressed as follows

$$\tau = -\frac{1}{\pi}\sum_{n=0}^{\infty}(c_{44}a_n + e_{15}b_n)Q_n H_n(b,x), \tag{43}$$

$$D = \frac{1}{\pi}\sum_{n=0}^{\infty}(\varepsilon_{11}b_n - e_{15}a_n)Q_n H_n(b,x), \tag{44}$$

where

$$H_n(b,x) = -F_1(b,x,n), \qquad n = 0,1,2,3,4,5,\dots, \qquad (\text{for } 0 < x < b),$$

$$H_n(b,x) = (-1)^{n+1}F_2(b,x,n), \qquad n = 0,1,2,3,4,5,\dots, \qquad (\text{for } 1 < x),$$

$$F_1(b,x,n) = \frac{2(1-b)^{n+1}}{\sqrt{(1+b-2x)^2-(1-b)^2}[1+b-2x+\sqrt{(1+b-2x)^2-(1-b)^2}]^{n+1}},$$

$$F_2(b,x,n) = \frac{2(1-b)^{n+1}}{\sqrt{(2x-1-b)^2-(1-b)^2}[2x-1-b+\sqrt{(2x-1-b)^2-(1-b)^2}]^{n+1}}.$$

At the left tip of the right crack, we obtain the stress intensity factor $K_L$ as

$$K_L = \lim_{x\to b^-}\sqrt{2\pi(b-x)}\cdot\tau = \sqrt{\frac{2}{\pi(1-b)}}\sum_{n=0}^{\infty}(c_{44}a_n + e_{15}b_n)Q_n. \tag{45}$$

At the right tip of the right crack, we obtain the stress intensity factor $K_R$ as

$$K_R = \lim_{x\to 1^+}\sqrt{2\pi(x-1)}\cdot\tau = \sqrt{\frac{2}{\pi(1-b)}}\sum_{n=0}^{\infty}(-1)^n(c_{44}a_n + e_{15}b_n)Q_n. \tag{46}$$

At the left tip of the right crack, we obtain the electric displacement intensity factor $D_L$ as

$$D_L = \lim_{x\to b^-}\sqrt{2\pi(b-x)}\cdot D = \sqrt{\frac{2}{\pi(1-b)}}\sum_{n=0}^{\infty}(e_{15}a_n - \varepsilon_{11}b_n)Q_n. \tag{47}$$

At the right tip of the right crack, we obtain the electric displacement intensity factor $D_R$ as

$$D_R = \lim_{x\to 1^+}\sqrt{2\pi(x-1)}\cdot D = \sqrt{\frac{2}{\pi(1-b)}}\sum_{n=0}^{\infty}(-1)^n(e_{15}a_n - \varepsilon_{11}b_n)Q_n. \tag{48}$$

## 5. Numerical Calculations and Discussion

This section presents numerical results of several representative problems. Adopting the first 10 terms in the infinite series (35), we followed the Schmidt procedure. To check accuracy, the values of $\sum_0^9 a_n E_n(x)$ and $U(x)$ are given in Table 1 for $b = 0.5$, $h = 1.0$, $\lambda = 0.2$. In Table 2, the values of the coefficients $a_n$ are given for $b = 0.5$, $h = 1.0$, $\lambda = 0.2$. From the above results and literatures [see e.g., 34–36], it can be seen that the Schmidt method performs satisfactorily if the first ten terms of the infinite series (35) are retained. The solution does not change with an increase of the number of terms in (35) beyond 10. The precision of present solution can satisfy the demands of the practical problem. The solution of two collinear cracks of arbitrary length *a–b* can easily be obtained by a simple change in the numerical values of the present paper ($a > b > 0$), that is, it can use the results of the collinear cracks of length 1–*b*/*a* and the strip width *h*/*a* in the present paper. The solution of this paper is suitable for the arbitrary length two collinear cracks in the piezoelectric layer bonded to dissimilar half spaces. All applications were focused on two cracked piezoelectric layer bonded to half planes. The piezoelectric layer is assumed to be the commercially available piezoelectric PZT-4 or PZT-5H, and the half planes are either aluminum or epoxy. The engineering material constants are listed in Table 3 [25]. The results of the present paper are shown in Figures 2–7, respectively. From the results, the following observations are very significant:

(1) The stress intensity factors not only depend upon the crack length, the electric loading and the width of the piezoelectric layer, but also on the properties of the materials.
(2) The interaction of the two collinear cracks decrease when the distance between the two collinear cracks increases.
(3) The stress intensity factors decrease when the width of the piezoelectric layer increases, and the results of the inner crack tips are bigger than at the outer crack tips.
(4) The solutions of this paper are approximate to ones of two collinear Griffith cracks in infinite piezoelectric materials for width $h \geqslant 3.5$, that is the influence of the width of the piezoelectric layer to the results is small when $h \geqslant 3.5$.
(5) The influence of the electric loading to the results is large for a thin piezoelectric layer, but not for a thick layer. This is consistent with the conclusion that the stress intensity factor is independent on the electric loading for infinite piezoelectric materials.

*Table 1.* Values of $\sum_0^9 a_n E_n(x)/(\pi\tau_0(1+\lambda)/2\mu)$ and $U(x)/(\pi\tau_0(1+\lambda)/2\mu) = x - b$ for $b = 0.5$, $h = 1.0$, $\lambda = 0.2$

| $x$ | $\sum_0^9 a_n E_n(x)/(\pi\tau_0(1+\lambda)/2\mu)$ | $U(x)/(\pi\tau_0(1+\lambda)/2\mu) = x - b$ |
|---|---|---|
| 0.5 | 0.0000 | 0.0000 |
| 0.6 | 0.1001 | 0.1000 |
| 0.7 | 0.1999 | 0.2000 |
| 0.8 | 0.2999 | 0.3000 |
| 0.9 | 0.4001 | 0.4000 |

*Table 2.* Values of $a_n/(\pi\tau_0(1+\lambda)/2\mu)$ for $b=0.5$, $h=1.0$, $\lambda=0.2$

| $n$ | $a_n/(\pi\tau_0(1+\lambda)/2\mu)$ |
|---|---|
| 0 | 0.163686E + 00 |
| 1 | 0.358555E − 03 |
| 2 | 0.192953E − 04 |
| 3 | 0.253487E − 05 |
| 4 | 0.376789E − 06 |
| 5 | 0.257585E − 07 |
| 6 | 0.312511E − 08 |
| 7 | 0.260541E − 09 |
| 8 | 0.354621E − 10 |
| 9 | 0.434612E − 11 |

*Table 3.* Material properties used in the examples

| | Piezoelectric layer | | | Elastic half plane | |
|---|---|---|---|---|---|
| | PZT-4 | PZT-5H | | Aluminum | Epoxy |
| $c_{44}$ $(\times 10^{10} N/m^2)$ | 2.56 | 2.3 | $c_{44}^E$ | 2.65 | 0.176 |
| $e_{15}$ $(c/m^2)$ | 12.7 | 17.0 | | 0 | 0 |
| $\varepsilon_{11}$ $(\times 10^{-10} c/Vm^2)$ | 64.6 | 150.4 | | – | – |

(6) The stress intensity factor becomes small with increasing electric loading. In other words, the electric field will reduce the magnitude of the stress intensity factor. This is due to the coupling between the electric and the mechanical fields. It can be shown from the Figures 2, 3, 4.

(7) The stress and electric displacement intensity factors become small with the decreasing of the crack's length.

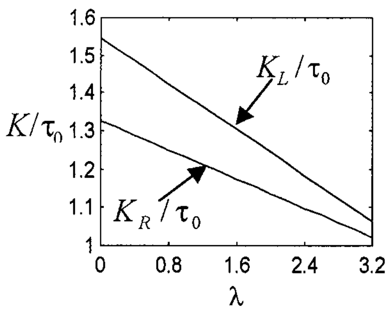


*Figure 2.* Stress intensity factors versus $\lambda$ for $b = 0.1$, $h = 0.6$ (Aluminum /PZT-5H/ Aluminum).

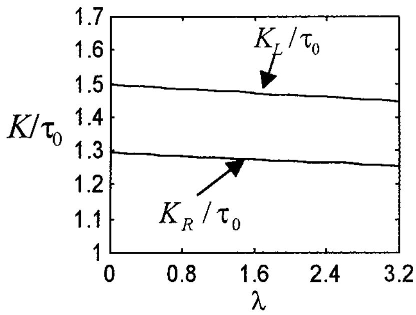


*Figure 3.* Stress intensity factors versus $\lambda$ for $b = 0.1$, $h = 2.5$ (Aluminum /PZT-5H/ Aluminum).

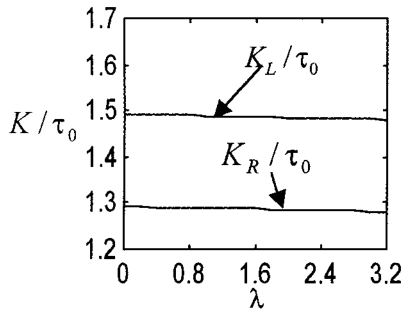


*Figure 4.* Stress intensity factors versus $\lambda$ for $b = 0.1$, $h = 5.0$ (Aluminum /PZT-5H/ Aluminum).

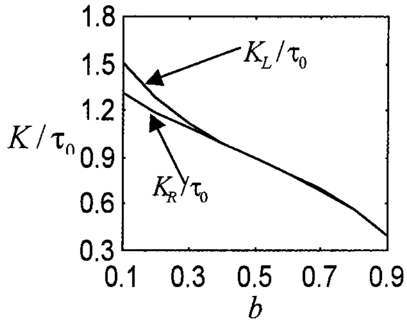


*Figure 5.* Stress intensity factors versus $b$ for $\lambda = 0.2$, $h = 0.5$ (Aluminum /PZT-5H/ Aluminum).

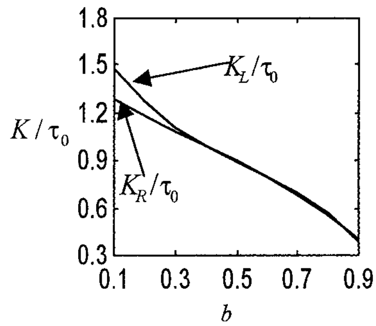


*Figure 6.* Stress intensity factors versus $b$ for $\lambda = 0.2$, $h = 3.5$ (Aluminum /PZT-5H/ Aluminum).

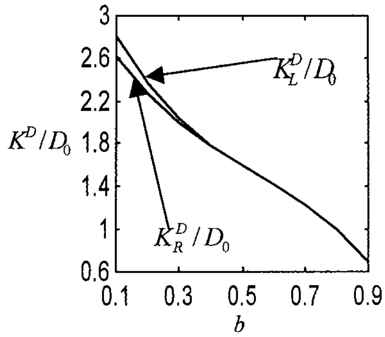


*Figure 7.* Electric intensity factors versus $b$ for $\lambda = 0.2$, $h = 1.0$ (Aluminum /PZT-5H/ Aluminum).


## Acknowledgements

The authors are grateful for financial support from the Post Doctoral Science Foundation of Hei Long Jiang Province, the Natural Science Foundation of Hei Long Jiang Province, the National Science Foundation with Excellent Young Investigators Award and the Scientific Research Foundation of Harbin Institute of Technology (HIT.2000.30).


## References


1. Deeg, W.E.F., *The Analysis of Dislocation, Crack and Inclusion Problems in Piezoelectric Solids*, Ph.D. thesis, Stanford University, 1980.
2. Pak, Y.E., 'Crack extension force in a piezoelectric materials', *ASME J. Appl. Mech.* **57** (1990) 647–653.
3. Pak, Y.E., 'Linear electro-elastic fracture mechanics of piezoelectric materials', *Int. J. Fract.* **54** (1992) 79–100.
4. Sosa, H.A. and Pak, Y.E., 'Three-dimensional eigenfunction analysis of a crack in a piezoelectric ceramics', *Int. J. Solids Struct.* **26** (1990) 1–15.
5. Sosa, H., 'Plane problems in piezoelectric media with defects', *Int. J. Solids Struct.* **28** (1991) 491–505.
6. Sosa, H., 'On the fracture mechanics of piezoelectric solids', *Int. J. Solids Struct.* **29** (1992) 2613–2622.
7. Suo, Z., Kuo, C.-M., Barnett, D.M. and Willis, J.R., 'Fracture mechanics for piezoelectric ceramics', *J. Mech. Phys. Solids* **40** (1992) 739–765.
8. Gao, H., Zhang, T.Y. and Tong, P., 'Local and global energy rates for an elastically yielded crack in piezoelectric ceramics', *J. Mech. Phys. Solids* **45** (1997) 491–510.
9. Li, X.F., Fan, T.Y. and Wu, X.F., 'A Moving mode-III crack at the interface between two dissimilar piezoelectric materials', *Int. J. Engng. Sci.* **38** (2000) 1219–1234.
10. Chen, Z.T., Karihaloo, B.L. and Yu, S.W., 'A Griffith crack moving along the interface of dissimilar piezoelectric materials', *Int. J. Fracture* **91** (1998) 197–203.
11. Chen, Z.T. and Karihaloo, B.L., 'Dynamic response of a cracked piezoelectric ceramic under arbitrary electro-mechanical impact', *Int. J. Solids Struct.* **36** (1999) 5125–5133.
12. Yu, S.W. and Chen, Z.T., 'Transient response of a cracked infinite piezoelectric strip under anti-plane impact', *Fatigue Engng. Mater. Struct.* **21** (1998) 1381–1388.
13. Sosa, H. and Khutoryansky, N., 'Transient dynamic response of piezoelectric bodies subjected to internal electric impulses', *Int. J. Solids Struct.* **36** ( 1999) 5467–5484.
14. Zhang, T.Y. and Hack, J.E., 'Mode-III cracks in piezoelectric materials', *J. Appl. Phys.* **71** (1992) 5865–5870.
15. McMeeking, R.M., 'On mechanical stress at cracks in dielectrics with application to dielectric breakdown', *J. Appl. Phys.* **62** (1989) 3316–3122.
16. Suo, Z., 'Models for break-down resistant dielectric and ferroelectric ceramics', *J. Mech. Phys. Solids* **41** (1993) 1158–1176.
17. Dunn, M.L., 'The effects of crack face boundary conditions on the fracture mechanics of piezoelectric solids', *Engng Fract. Mech.* **48** (1994) 38–94.

18. Zhang, T.Y. and Tong, P., 'Fracture mechanics for a mode III crack in a piezoelectric material', *Int. J. Solids Struct.* **33** (1996) 343–359.
19. Sosa, H. and Khutoryansky, N., 'New developments concerning piezoelectric materials with defects', *Int. J. Solids Struct.* **33**(23), (1996) 3399–3414.
20. Tauchert, T.R., 'Cylindrical bending of hybrid laminates under thermo-electro-mechanical loading', *J. Thermal Stresses* **19** (1996) 287–298.
21. Lee, J.S. and Jiang, L.Z., 'Exact electro-elastic analysis of piezoelectric laminate via state space approach', *Int. J. Solids Struct.* **33** (1996) 977–989.
22. Batra, R.C. and Liang, X.Q., 'The vibration of a rectangular laminated elastic plate with embedded piezoelectric sensors and actuators', *Comput. Struct.* **63** (1997) 203–215.
23. Heyliger, P., 'Exact solutions for simply supported laminated piezoelectric plates', *ASME J. Appl. Mech.* **64** (1997) 299–311.
24. Shindo, Y., Domon, W. and Narita, F., 'Dynamic bending of a symmetric piezoelectric laminated plate with a through crack', *Theor. Appl. Fract. Mech.* **28** (1998) 175–186.
25. Narita, K., Shindo, Y. and Watanabe, K., 'Anti-plane shear crack in a piezoelectric layered to dissimilar half spaces', *JSME Int. J.*, Series A **42** (1999) 66–72.
26. Morse, P.M. and Feshbach, H., *Methods of Theoretical Physics*, Vol. 1, McGraw-Hill, New York, 1958, pp. 925–937.
27. Wang, B., 'Three dimensional analysis of a flat elliptical crack in a piezoelectric materials', *Int. J. Engng. Sci.* **30**(6) (1992) 781–791.
28. Park, S.B. and Sun, C.T., 'Effect of electric field on fracture of piezoelectric ceramics', *Int. J. Fract.* **70** (1995) 203–216.
29. Han, Xue-Li and Wang, Tzuchiang, 'Interacting multiple cracks in piezoelectric materials', *Int. J. Solids Struct.* **36** (1999) 4183–4202.
30. Narita, K. and Shindo, Y., 'Anti-plane shear crack growth rate of piezoelectric ceramic body with finite width', *Theor. Appl. Fract. Mech.* **30** (1998) 127–132.
31. Gradshteyn, I.S. and Ryzhik, I.M., *Table of Integral, Series and Products*, Academic Press, New York, 1980, pp. 1025–1031.
32. Erdelyi, A. (ed), *Tables of Integral Transforms*, McGraw-Hill, New York, 1954, Vol. 1, pp. 101–128.
33. Amemiya, A. and Taguchi, T., *Numerical Analysis and Fortran*, Maruzen, Tokyo, 1969, pp. 346–372.
34. Itou, S., 'Three dimensional waves propagation in a cracked elastic solid', *ASME J. Appl. Mech.* **45** (1978) 807–811.
35. Zhou, Z.G., Bai, Y.Y. and Zhang, X.W., 'Two collinear Griffith cracks subjected to uniform tension in infinitely long strip', *Int. J. Solids Struct.* **36** (1999a) 5597–5609.
36. Zhou, Z.G., Han, J.C. and Du, S.Y., 'Investigation of a Griffith crack subject to anti-plane shear by using the non-local theory', *Int. J. Solids Struct.* **36** (1999b) 3891–3901.